Optical true time-delay for two-dimensional phased array antennas using compact fiber grating prism

Yongfeng Wei (魏永峰)[1,4], Chaowei Yuan (袁超伟)[1], Shanguo Huang (黄善国)[2*], Xinlu Gao (高欣璐)[3], Jing Zhou (周 静)[3], Xi Han (韩 曦)[1], and Wanyi Gu (顾畹仪)[2]

[1]*School of Information and Communication Engineering, Beijing University of Posts and Telecommunications, Beijing 100876, China*

[2]*State Key Laboratory of Information Photonics and Optical Communications, Beijing University of Posts and Telecommunications, Beijing 100876, China*

[3]*Department of Physics, Beijing Normal University, Beijing 100875, China*

[4]*Department of Electronic Information Engineering, Inner Mongolia University, Hohhot 010021, China,*

[*]*Corresponding author: shghuang@bupt.edu.cn*

Received May 27, 2013; accepted September 4, 2013; posted online September 29, 2013

A two-dimensional (2D) optical true-time delay (TTD) beam-forming system using a compact fiber grating prism (FGP) for a planar phased array antenna (PAA) is proposed. The optical beam-forming system mainly consists of a TTD unit based on the same compact FGP, one tunable laser for elevation beam steering, and a controlled wavelength converter for azimuth beam steering. A planar PAA using such 2D optical TTD unit has advantages such as compactness, low bandwidth requirement for tunable laser sources, and potential for large-scale system implementations. The proof-of-concept experiment results demonstrate the feasibility of the proposed scheme.

OCIS codes: 060.3735, 060.4510.

doi: 10.3788/COL201311.100606.

True time-delay (TTD) beam forming for phased array antennas (PAAs) has been investigated extensively over the past few years. Optically controlled TTD beam-forming systems potentially have a number of important advantages, such as small size, light weight, low propagation loss, immunity to electromagnetic interference (EMI), remoting capability, simplified transmitting/receiving architectures and squint-free beam scanning over a broad frequency range, over their electrical beam-forming counterparts[1]. Various approaches for TTD beam-forming have been proposed and demonstrated; the earliest TTD systems make use of fixed-length optical fiber delay lines[2] and subsequent TTD systems incorporated high dispersive fibers to form a fiber-optic prism[3], discrete fiber Bragg gratings (FBGs)[4,5], chirped fiber gratings (CFGs)[6–9], piezoelectric fiber stretchers[10], and photonic crystal fibers (PCFs)[11]. Most of the architecture mentioned above focused on the realization of TTD for 1D beam steering. The ability of the beam-forming network to support two-dimensional (2D) arrays for practical applications is required. A 2D planar PAA has a pencil-shaped radiation pattern that can scan the main beam toward any direction in space with higher gain. A few architectures have been proposed, and have demonstrated the implementation of a 2D optical TTD beam-forming system[12–17]. In Refs. [15,16], an optical TTD architecture that combined wavelength-dependent and wavelength-independent time delay units was proposed to achieve 2D beam-forming system. In Ref. [17], the TTD module size was proportionally reduced by using PCFs to increase dispersion. A seven-bit photonic TTD system that used an 8×8 optical switch for PAA beam formation was proposed in Ref. [18]. In Ref. [19], the wavelength-dependent unit was a continuously tunable TTD network based on a high dispersed photonic bandgap fiber that could effectively reduce the length of fibers. All these architectures consisted of a large number of optical switches. For a large-sized 2D planar PAA, more optical switches are required, and the consequent insertion and nonuniform losses in the delay line are higher.

In this letter, we propose a novel 2D optical TTD beam-forming system that uses a series of similar compact fiber grating prisms (FGPs) in which the time delays are created by the reflections from two opposite directions of the FBGs. Therefore, the system is more compact and has less optical switches. The bandwidth requirement for the tunable laser source (TLS) is significantly reduced as well. The proof-of-concept experiment results demonstrate the feasibility of the proposed scheme.

Figure 1 shows the configuration of the proposed 2D optical TTD beam-forming system for a PAA with $N \times N$ radiating elements. The system is composed of three

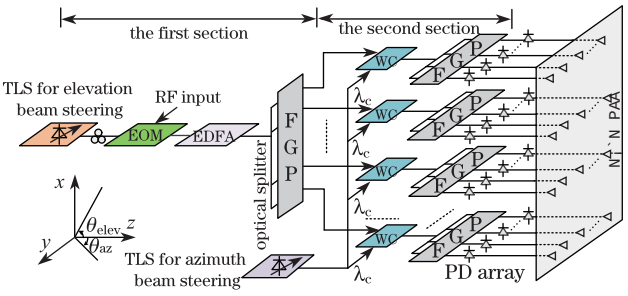

Fig. 1. (Color online) Schematic of the proposed 2D optical TTD beam-forming system.

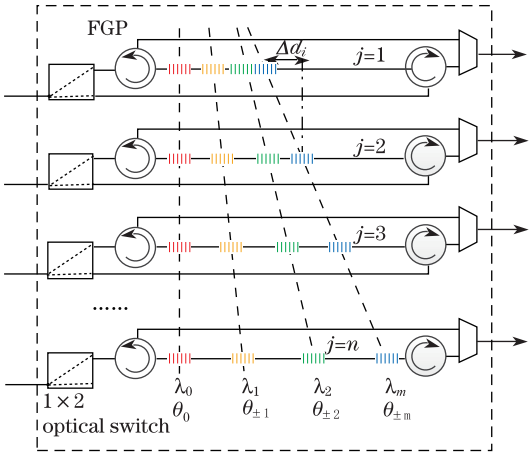

Fig. 2. (Color online) Configuration of the compact FGP using discrete FBGs.

sections. The first section is the TTD for elevation beam steering, which consists of TLS, electro-optic modulator (EOM), erbium-doped fiber amplifier (EDFA), optical splitter, and compact FGP. The second section is the TTD for azimuth beam steering, which includes N wavelength conversion devices (WCs), N compact FGPs, corresponding optical amplifier, and splitter devices. The last section consists of $N \times N$ photo-detector (PD) array and PAA. Light with a certain wavelength generated by the TLS for elevation beam steering first passes through a polarization controller (PC) and then modulated by the radio frequency (RF) signal at the EOM. The RF signal is applied to all optical channels through the EOM. The modulated light is amplified by the EDFA and then fed into the $1:N$ equal path optical splitter. The split lights are injected into the TTD unit using the compact FGP for beam steering in the elevation plane. By tuning the optical wavelength of the TLS for elevation beam steering, the relative delay of the signals in the x dimension is changed. Then, the N delayed lights are fed to the same N devices of wavelength conversion controlled by the TLS for azimuth beam steering. After wavelength conversion, N optical channels are connected to the N optical TTD units using the same compact FGP for beam steering in the azimuthal plane. By tuning the optical wavelength of the TLS for azimuth beam steering, the relative delay of the signals in the y dimension is changed. Afterward, we can obtain the appropriate time delays by tuning the two TLSs. The $N \times N$ PD array recovers the time-delayed RF signals that are post-amplified and fed to $N \times N$ antenna elements. Finally, a planar PAA with $N \times N$ antenna elements is formed using the 2D optical TTD beam-forming system that uses $N+1$ compact FGPs.

The configuration of the compact FGP used in the 2D optical TTD beam-forming system we previously reported in Ref. [20], is illustrated in Fig. 2. The prism is constructed using n fiber delay lines. The m uniform FBGs with different center wavelengths λ_m are written at different locations of every fiber delay line. Every fiber delay line is connected to the optical circulators at each end. Light from the optical splitter could enter the time delay line from either left or right by adjusting the 1×2 optical switch. Then, the light in each delay line is reflected from different positions in different fiber delay lines and produces different round trip time delays. Each dashed line corresponds to a Bragg wavelength and shows the reflection positions schematically in Fig. 2. Therefore, each wavelength is associated with $2n$ different roundtrip time delays created by the n fiber delay lines.

In Fig. 2, Δd_i represents the position difference between the FBGs with the same Bragg wavelength λ_i at adjacent time delay fibers. In this situation, the time delay difference caused by λ_i in adjacent time delay fibers is given by

$$\Delta\tau_i = \frac{2n_{\text{eff}}\Delta d_i}{c} \cdot S, \tag{1}$$

where $S = \pm 1$ is the state of the optical switch, n_{eff} is the effective refractive index of the fiber, and c is the speed of light in free space. Equation (1) indicates that the increment of $\Delta\tau_i$ can vary by tuning λ_i of the TLS, and each λ_i is associated with two opposite roundtrip time delays when the optical switches are all in cross state ($S = 1$) or bar state ($S = -1$). Using the configuration of the compact FGP to generate the x and y dimension time delays, we can construct a 2D optical TTD beam-forming system for planar PAAs. The λ_i signal experiences a time delay in the first section of the 2D TTD to obtain the desired elevation angle of the radiation beam by tuning the wavelength of the TLS. For an array element spacing of d_x along x axis, the desired elevation angle θ_{elev} is given by

$$\theta_{\text{elev}} = \sin^{-1}\left(\frac{c \cdot \Delta\tau_x}{d_x}\right), \tag{2}$$

where $\Delta\tau_x$ is the time-delay difference in x direction.

Then, the N time-delayed signals from the FGP in the first section are converted to λ_c by N wavelength conversion devices. The desired azimuth angle of the radiation beam can be obtained by tuning λ_c of the TLS to control the wavelength conversion device. For an array element spacing of d_y along y axis, the desired azimuth angle θ_{az} is expressed as

$$\theta_{\text{az}} = \sin^{-1}\left(\frac{c \cdot \Delta\tau_y}{d_y}\right), \tag{3}$$

where $\Delta\tau_y$ is the time-delay difference in y direction.

Equations (2) and (3) indicate the squint-free beaming-steering operation of optical TTD systems. The steering angles in elevation plane θ_{elev} and in azimuthal plane θ_{az} are related to the time-delay differences controlled by the two TLSs. If the antenna elements are homogeneously excited, the far-field distribution by the $N \times N$ antenna

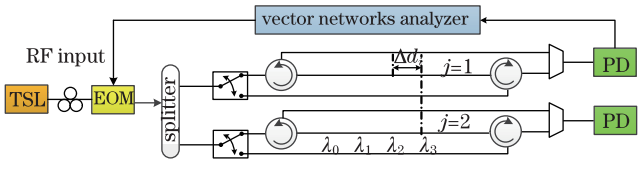

Fig. 3. (Color online) Experimental setup for the time-delay difference measurement. This setup is also used for the time-delay measurement in the 2D optical TTD.

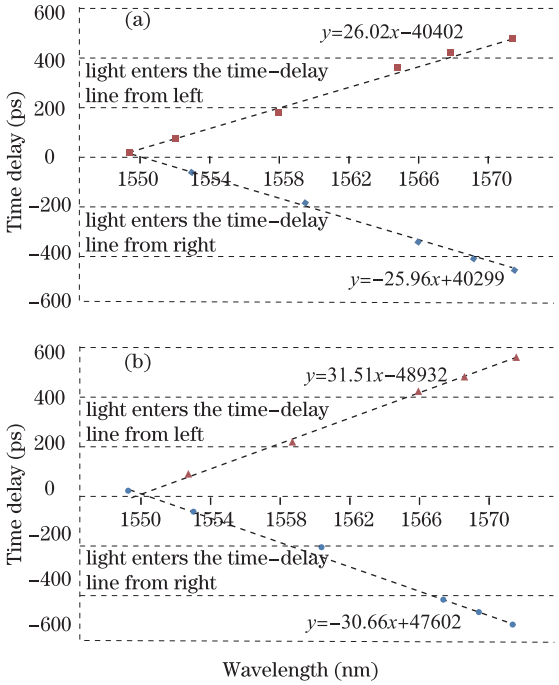

Fig. 4. (Color online) Measured time delay curves of the compact FPG: (a) first time-delay line in the compact FGP; (b) second time-delay line in the compact FGP.

elements can be expressed as

$$E(\theta_{\rm az},\theta_{\rm elev}) = E_x(\theta_{\rm az},\theta_{\rm elev})\cdot E_y(\theta_{\rm az},\theta_{\rm elev}) = \left(\sum_{m=1}^{N} {\rm e}^{{\rm j}(m-1)kd_x\sin(\theta_{\rm az})\sin(\theta_{\rm elev})}\right)\cdot \left(\sum_{n=1}^{N} {\rm e}^{{\rm j}(n-1)kd_y\sin(\theta_{\rm az})\cos(\theta_{\rm elev})}\right), \quad (4)$$

where k is the wave number of the RF signal. For example, to scan in $(\theta_{\rm az0},\theta_{\rm elev0})$ direction, the x dimension time-delay interval can be provided by one FGP in the first section. Similarly, the y dimension time-delay interval can be provided by N FGPs in the second section. Therefore, the proposed 2D optical TTD beam-forming system using compact FGP modules can provide a discrete beam steering of a planar PAA. Wavelength conversion that transfers time delay information successfully from one wavelength to another can eliminate optical/electrical/optical conversion loss. This conversion results in an ultra-compact system with low complexity and low bandwidth requirement for TLSs, as well as with a potential for large-scale system implementations.

The foundation of a compact FGP architecture involves time delay lines that could provide the required time delays when lights enter the FBG from either the left or right direction. Moreover, the architecture can be expediently extended to a 2D beam-forming system by cascading the compact FGPs using wavelength conversion. To prove such concept, an optical TTD for a planar PAA is experimentally investigated. Figure 3 shows the setup for the measurement of the time-delays of the compact FGP using two FBG time-delay lines with 12 discrete FBGs. However, only six pairs of FBGs in the two FBG time delay lines have the same Bragg wavelengths, namely, 1552.128, 1554.062, 1559.852, 1565.920, 1567.960, and 1569.999 nm. In addition, each FBG has a length of 10 mm, a full-width at half-maximum (FWHM) bandwidth of about 0.2 nm, and a peak reflectivity of higher than 90%.

The light from the tunable laser (AQ4321A, Ando, Japan) is sent to the EOM through the polarization controller. The RF signal with a frequency of 15.01 GHz from the network analyzer (8722ES, Agilent, USA) is amplified to 27 dBm using a microwave amplifier (JSM-KFD76C) and then applied to the modulator. The light, which is split into two beams, can enter the compact FGP consisting of two FBG time-delay lines. In the compact FGP, the light can enter the FBG time-delay lines from either left or right by adjusting the 1×2 optical switch to bar or cross state. The delayed signals are then detected by high-speed PDs (XPDV3120R-VF-FP, u^{2}t Photonics AG, Germany) with 3-dB bandwidth of 70 GHz. The amplitude and phase of the detected RF signal are measured by the network analyzer, and the corresponding TTD performance can be analyzed. Calibrating all the time-delay lines of the system before operation is important.

By turning the light wavelength on 1552.128, 1554.062, 1559.852, 1565.920, 1567.960, and 1569.999 nm, the time delays of the six channels in the two time delay lines are measured. The 1552.128 nm wavelength is selected as a reference for zero time delay. The measured average time-delay difference and the desired angle in the situation of $d_x = d_y = \lambda_{\rm 5GHz}/2$ are shown in Table 1. Results show that the two time delay lines have a time-delay response regardless of the direction the light comes from. The experimentally measured time-delay curves are shown in Fig. 4, and the fitting formulas displayed beside the curves show that the two fitting curves have nearly the same absolute slopes whether light enters the time-delay lines from the left or the right port. The differences in the absolute slopes may be due to the inaccurate position of the corresponding FBG in the two time delay lines, the uncertainty of the optical source, and the errors in the measurement.

A 2D optical TTD beam-forming system is formed by cascading the compact FGPs using wavelength conversion, as shown in Fig. 1. Suppose the frequency of RF signal is 5 GHz and $\Delta\tau_i$ is positive, by turning the light wavelength of the TLS for elevation beam steering on 1552.128 nm, the azimuth beam steering angles are 2.22°, 11.4°, 32.6°, 37.2°, and 66.8° when the light wavelengths

Table 1. Time-delay Difference Measurement of Compact FGP in Different Switch-states

Bragg Wavelength (nm)	Time-delay Difference (ps) -Switch States		Desired Angle (deg.) -Switch States	
	All in cross	All in bar	All in cross	All in bar
1552.128	0	0	0	0
1554.062	3.9	–3.8	2.22	–2.24
1559.852	19.7	–19.0	11.4	–11.0
1565.920	53.9	–54.1	32.6	–32.8
1567.960	60.4	–61.2	37.2	–37.7
1569.999	91.9	–91.3	66.8	–65.9

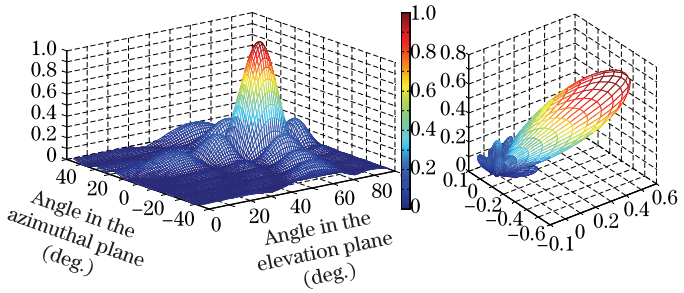

Fig. 5. (Color online) Simulated gain pattern of the PAA when $\theta_{\mathrm{elev}} = 11.4°$ and $\theta_{\mathrm{az}} = 66.8°$

of the TLS for azimuth beam steering are turned on 1554.062, 1559.852, 1565.920, 1567.960, and 1569.999 nm, respectively. A different beam can radiate in the desired direction by turning the TLS for elevation beam steering and for azimuth beam steering simultaneously. The normalized far-field patterns are simulated with the designed time delay values. When the angle in the elevation plane $\theta_{\mathrm{elev}} = 11.4°$, a time delay of 19.7 ps is generated by turning the TLS for elevation beam steering wavelength on 1559.852 nm. When the angle in the azimuthal plane $\theta_{\mathrm{az}} = 66.8°$, a time delay of 91.9 ps is generated by turning the TLS for azimuth beam steering wavelength on 1569.999 nm. The simulated pattern of the 10×10 PAA based on the measured time delay values is shown in Fig. 5. The three-dimensional plots clearly illustrate the designed steering angles.

In conclusion, a 2D optical TTD beam-forming system for a planar PAA using compact FGP, which has low bandwidth requirement for TLSs, is proposed. The proposed 2D optical TTD beam-forming system can greatly reduce the number and length of the FBGs, and has potential for large-scale system implementations. The proof-of-concept experiment results show the feasibility of this proposed optimized structure. The integration of beam-forming functions using monolithic integration[21] and silicon photonic integration technologies[22] will further reduce the size, energy consumption, and cost of the optical TTD beam-forming system.

This work was supported by the National "973" Project of China (Nos. 2010CB328202, 2010CB328204, and 2012 CB315604), the National Natural Science Foundation of China (Nos. 61271191 and 61001124), the National "863" Project of China (No. 2012AA011302), the Program for New Century Excellent Talents in University (No. NCET-12-0793), the Beijing Nova Program (No. 2011065), and the Fundamental Research Funds for the Central Universities.

References

1. J. Capmany and D. Novak, Nature Photon. **1,** 319 (2007).
2. W. Ng, A. A. Walston, G. L. Tangonan, J. J. Lee, I. L. Newberg, and N. Bernstein, J. Lightwave Technol. **9,** 1124 (1991).
3. R. D. Esman, M. Y. Frankel, J. L. Dexter, L. Goldberg, M. G. Parent, D. Stilwell, and D. G. Cooper, IEEE Photon. Technol. Lett. **5,** 1347 (1993).
4. A. Molony, C. Edge, and I. Bennion, Electron. Lett. **31,** 1485 (1995).
5. S. Huang, J. Li, Y. Ye, P. Shi, J. Zhou, B. Guo, and W. Gu, Opt. Laser Technol. **44,** 776 (2012).
6. J. L. Cruz, B. Ortega, M. V. Andres, B. Gimeno, D. Pastor, J. Capmany, and L. Dong, Electron. Lett. **33,** 545 (1997).
7. B. Ortega, J. L. Cruz, J. Capmany, M. V. Andres, and D. Pastor, IEEE J. Microw. Theory Tech. **48,** 1352 (2000).
8. Y. Liu, J. Yao, and J. Yang, Opt. Commun. **207,** 177 (2002).
9. D. B. Hunter, M. E. Parker, and J. L. Dexter, IEEE Trans. Microw. Theory Tech. **54,** 861 (2006).
10. D. A. Henderson, C. Hoffman, R. Culhane, and D. Viggiano III, Proc. SPIE **5589,** 99 (2004).
11. H. Subbaraman, M. Y. Chen, and R. T. Chen, J. Lightwave Technol. **26,** 2803 (2008).
12. D. Dolfi, F. Michel-Gabriel, S. Bann, and J. P. Huignard, Opt. Lett. **16,** 255 (1991).
13. M. Y. Frankel, P. J. Matthew, and R. D. Esman, IEEE Trans. Microw. Theory Technol. **44,** 2696 (1996).
14. D. T. K. Tong and M. C. Wu, IEEE Trans. Microw. Theory Tech. **46,** 108 (1998).
15. B.-M. Jung, J.-D. Shin, and B.-G. Kim, IEEE Photon. Technol. Lett. **19,** 877 (2007).
16. B.-M. Jung and J. Yao, IEEE Photon. Technol. Lett. **21,** 627 (2009).
17. Y. Jiang, Z. Shi, B. Howley, X. Chen, M. Y. Chen, and R. T. Chen, Opt. Eng. **44,** 125001 (2005).
18. Y. Yang, Y. Dong, D. Liu, H. He, Y. Jin, and W. Hu, Chin. Opt. Lett. **7,** 118 (2009).
19. M. Y. Chen, J. Lightwave Technol. **31,** 910 (2013).
20. C. Fan, S. Huang, X. Gao, J. Zhou, W. Gu, and H. Zhang, Opt. Fiber Technol. **19,** 60 (2013).
21. X. Fan, Y. Huang, X. Ren, X. Duan, F. Hu, and Q. Wang, Chin. Opt. Lett. **10,** 110402 (2012).
22. Z. Zhou, Z. Tu, B. Yin, W. Tan, L. Yu, H. Yi, and X. Wang, Chin. Opt. Lett. **11,** 012501 (2013).